ChemPhysChem

Supporting Information

Elucidating 2D Charge-Density-Wave Atomic Structure in an MX–Chain by the 3D-ΔPair Distribution Function Method**

Laurent Guérin,* Takefumi Yoshida,* Edoardo Zatterin, Arkadiy Simonov, Dmitry Chernyshov, Hiroaki Iguchi, Bertrand Toudic, Shinya Takaishi, and Masahiro Yamashita

Halogen-bridged Metal complexes (MX-Chains)

MX-Chain compounds are synthetic materials with general formula $[ML_2X]A_2$, where:

- M is a metal atom; M = (Ni ,Pd ,Pt)
- X is a halogen atom; X = (Cl, Br, I)
- L is a ligand coordinated with M containing amino groups (NH_2-)
- A is a counterion which is hydrogen-bonded to the amino group in L

The structure of an example MX-Chain compound is shown in Figure S1. The metal atom is coordinated with the amino-containing ligands L, to form a M-L monomer unit. All such units are bonded to a halogen atom to form a one-dimensional chain, -M-X-M-X-M-. The hydrogen bond which forms between the amino group of the ligands and the counterion A provides means of interchain cohesion, but in one orthogonal direction only. Bonding along the chain axis occurs by overlap of the dz^2 metal and pz halogen orbitals.

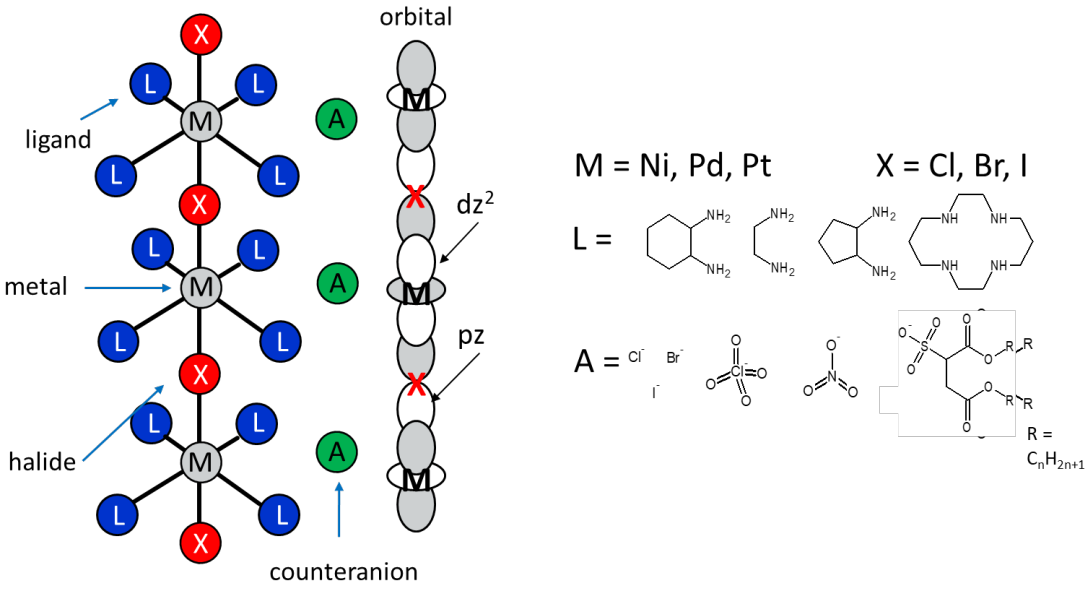

Figure S1. Structure of MX-Chain compounds.

Electronic ground state

The ground state of a system corresponds to its most energetically stable configuration in a given condition. MX chains can adopt two different electronic ground states (i.e., configurations of the electronic structure) depending on the metal ion employed, as depicted in Figure S2:

. M = Ni gives rise to a Mott Hubbard (MH) state;

. M = Pt and Pd gives rise to a Charge Density Wave (CDW) state.

Ni^{3+} MH compounds

A Mott insulator (MI) is a material that displays insulating behavior despite band theory predicts it to be conducting. Mott insulators are usually oxides of Transition Metals characterized by a high degree of electron-electron (e-e) correlation in the valence band. Unlike in other metals, the energy associated with this correlation is high enough to stabilize a new ground state where the half-occupied valence band is split into a full valence and an empty conduction bands separated by a gap; the material is thus insulating. Such behavior is described with the Hubbard model: in the Hamiltonian that bears the same name, a so-called Coulomb repulsion term *U* accounts for the e-e correlation, while the electron-phonon interaction (*S*) is competed with Coulomb repulsion energy (*U*). The relative contributions of *U* and *S* to the Hamiltonian describe the metal-to-insulator transition, where the insulating phase is stabilized when $U > S$, i.e. when the e-e correlation is strong enough (for example, in cases of high pressure) and the valence band splits into Lower (LH) and Upper (UH) Hubbard bands. The formation of the MH state in Ni-containing MX-Chain compounds does not manifest itself only by an insulating behavior. The strong Coulomb repulsion felt by the valence electrons of Nickel makes the Ni ions adopt a valence state of 3+ along the whole chain, whereby only one electron per each atom occupies the dz^2 orbital.

The chemical formula of the compound is thus of the type $[M^{3+}L_2X^-]A_2^-$. The X^- halogen atoms are seen to occupy the midpoints between the Ni^{3+} ions along the chain.

Pd, Pt mixed valence CDW compounds

The Charge Density Wave (CDW) state consists in a periodic modulation of the electronic density surrounding the constituent atoms or molecules resulting from a distortion of the lattice. This is the aforementioned Peierls transition, i.e. a distortion caused by the electron-lattice interaction, quantized into an extended version of the Hubbard model (the Peierls-Hubbard Hamiltonian) as *S*. It was established that in MX-Chains the competition between the onsite Coulomb repulsion *U* of the Metal ion and the e-l interaction *S* drives the stabilization of one or the other state. Recall that bonding along the MX chain axis occurs by overlap of the $3dz^2$ Metal and pz Halogen orbitals. Nickel possesses a spatially small $3dz^2$ band as compared to Pd or Pt. The interaction of its valence electrons with the lattice is hence weaker compared to the onsite repulsion that they feel, i.e. for Ni $U > S$; the MH state is hence stabilized. Conversely, Pt and Pd possess a spatially large $4dz^2$ and $5dz^2$ band, respectively: the interaction of the electrons with the lattice is strong enough to drive a Peierls distortion and the formation of the CDW state - $S > U$. Therefore, the Peierls distortion that occurs because of the large e-l interaction S which characterizes Pd and Pt compounds manifests itself via a dimerization, i.e. a doubling of the periodicity along the MX chain axis. Such doubling stabilizes a mixed valence state where Pd^{2+}, Pt^{2+} and Pt^{4+}, Pd^{4+} ions alternate giving rise to long and short M-X distances respectively, in the fashion $–X…M^{2+}…X\text{-}M^{4+}\text{-}X…M^{2+}$…. The general formula of this compounds is thus $[M^{2+}L_2][M^{4+}L_2X_2]A_4$.

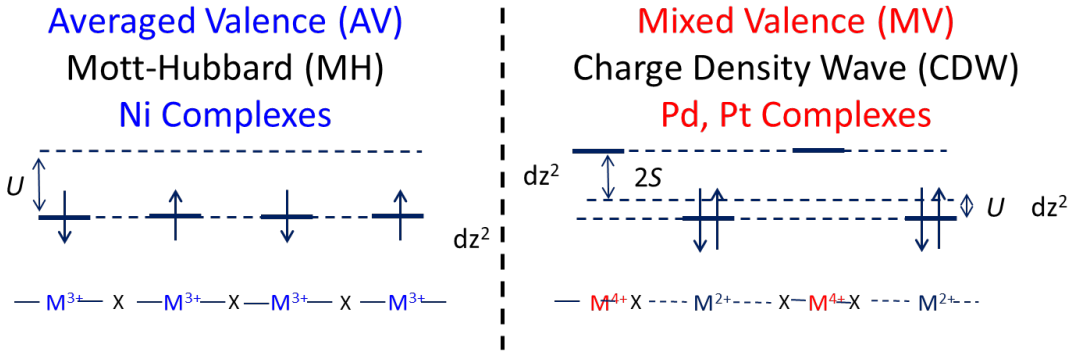

Figure S2. Electronic state of MX-Chain compounds

Average structure of $[Pd(cptn)_2Br]Br_2$

Data collection procedure and refinement are presented in the table S1.

Table S1. Crystal data of $[Pd(cptn)_2Br]Br_2$	
Chemical formula	$C_{10}H_{24}BrN_4Pd \cdot 2(Br)$
M_r	546.46
Crystal system, space group	Orthorhombic, *I*222
Temperature (K)	230
a, *b*, *c* (Å)	5.24672 (16), 6.9646 (3), 22.7002 (7)
V (Å^3)	829.49 (5)
Z	2
Radiation type	Cu *K*α
μ (mm^{-1})	17.41
Crystal size (mm)	0.37 × 0.23 × 0.05
Data collection	
Diffractometer	SuperNova, Single source at offset, EosS2
Absorption correction	Gaussian,*CrysAlis PRO*, Agilent Technologies, Version 1.171.37.35h (release 09-02-2015 CrysAlis171 .NET) (compiled Feb 9 2015,16:26:32) Numerical absorption correction based on gaussian integration over a multifaceted crystal model Empirical absorption correction using spherical harmonics, implemented in SCALE3 ABSPACK scaling algorithm.
T_{min}, T_{max}	0.042, 0.529
No. of measured, independent and observed [$I > 2\sigma(I)$] reflections	4909, 622, 621
R_{int}	0.085
θ_{max} (°)	59.8
$(\sin \theta/\lambda)_{max}$ (Å^{-1})	0.560
Refinement	
$R[F^2 > 2\sigma(F^2)]$, $wR(F^2)$, *S*	0.035, 0.093, 1.07
No. of reflections	622
No. of parameters	45
No. of restraints	6

H-atom treatment	H-atom parameters constrained
$\Delta\rho_{max}$, $\Delta\rho_{min}$ (e Å^{-3})	0.79, −1.15
Absolute structure	Flack x determined using 232 quotients [(I+)-(I-)]/[(I+)+(I-)] (Parsons, Flack and Wagner, Acta Cryst. B69 (2013) 249-259).
Absolute structure parameter	0.02 (3)

Computer programs: *CrysAlis PRO*, Agilent Technologies, Version 1.171.37.35h (release 09-02-2015 CrysAlis171 .NET) (compiled Feb 9 2015, 16:26:32), *SHELXL* (Sheldrick, 2008), Olex2 (Dolomanov *et al.*, 2009).

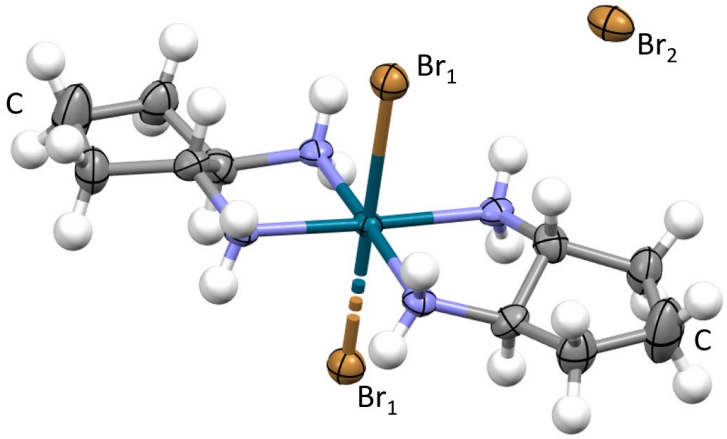

Figure S3. Molecular structure of $[Pd(cptn)_2Br]Br_2$. Duck blue: Pd; brown: Br; gray: C; white: H; purple: N.

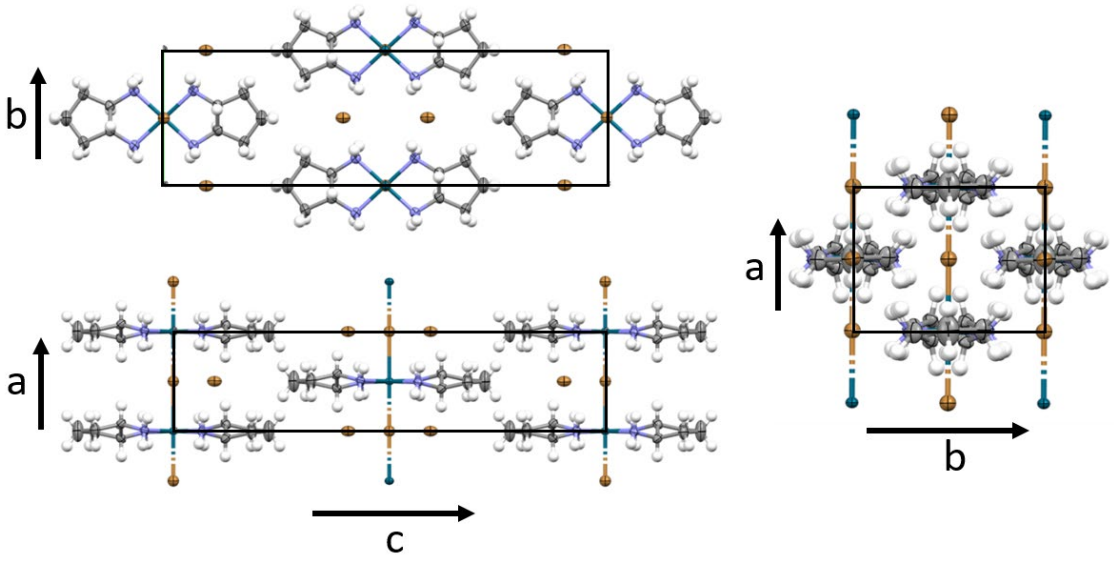

Figure S4. Crystal structure of $[Pd(cptn)_2Br]Br_2$.

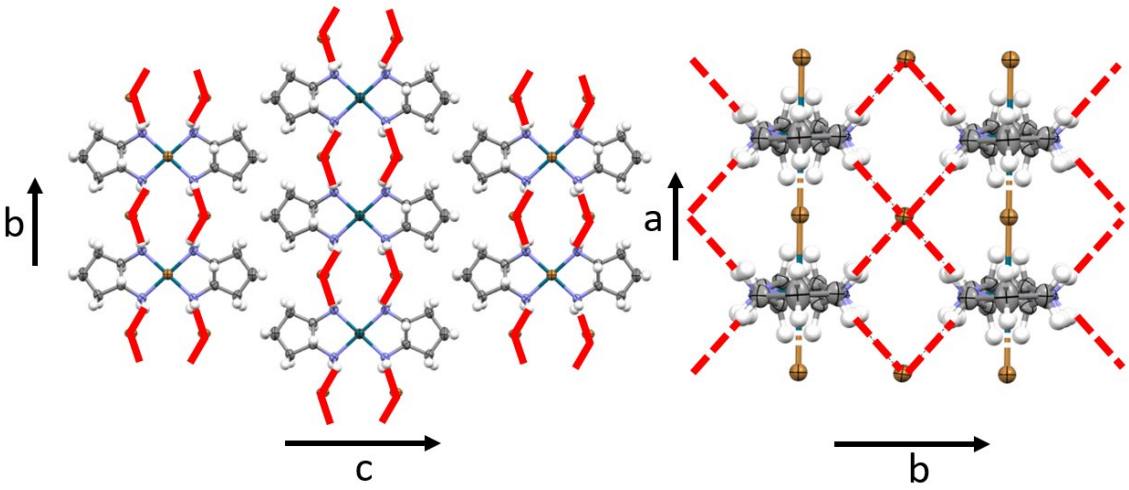

Figure S5. Hydrogen bonding of $[Pd(cptn)_2Br]Br_2$. The 1D MX chain runs along the *a* axis, so that the H-bond connects different chains along the *b* axis: no strong bonds are present in the *c* direction.

3D-ΔPDF model

How to read a 3D-ΔPDF map. The 3D-ΔPDF map has the same representation "problem" as Patterson map. The position of peaks corresponds to interatomic vectors. Although in the real structure this vector has its origin on the atom, in the ΔPDF its origin is always the origin of the unit cell. For example, in figure 4a, there is a positive peak at (0,0.2,0). This define an interatomic vector of coordinate (0,0.2,0). One has then to look in the average structure if there is an interatomic vector with this coordinate. This corresponds to the interatomic vector between Br2 and C in figure 4b. Notice that the Br2 atom is not at the center of the unit cell.

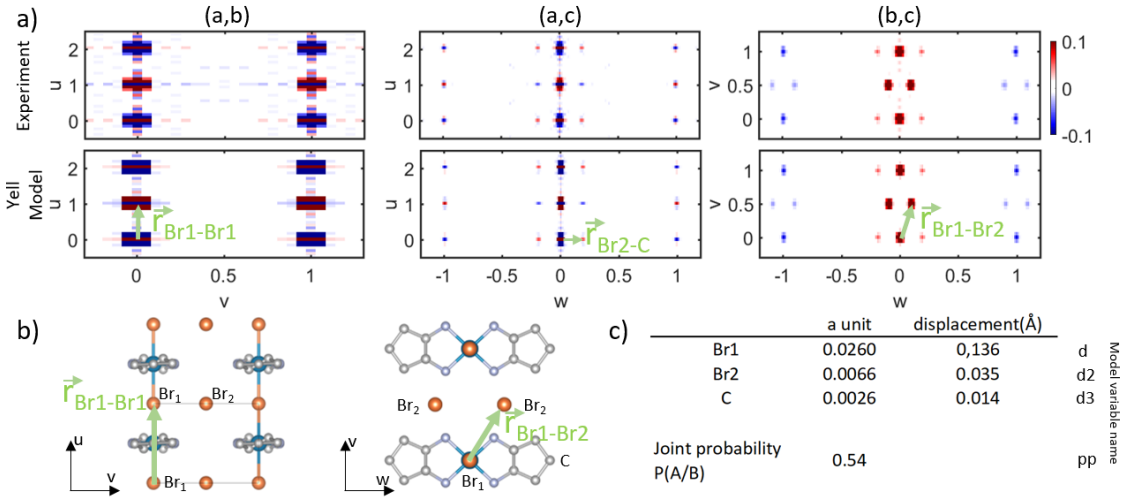

Figure S6. Result of the Yell model

Comparison with empirical model

A displacement of Δ = 0.136 Å of the Br bridging atom (Br1) along the chain is obtained. It has been established that the distortion parameter defined as $d = 2\Delta/a$, bears a linear relationship to a :

$d = 0.165\ a - 0.81$

The obtained value of $d = 0.052$ for $a = 5.25$ Å is in perfect agreement with other Pd-based MX chains found in a CDW state (Figure S7)

In the chain, U is affected by the electrostatic / ligand field around the dz^2 orbital. It appears that the influence of the axial ligand of Br anion is dominant, and the in-plane ligand of cptn is irrelevant. The ligand field affects the value of the on-site Coulomb repulsion U on the metal ion and stimulates the formation of the CDW mixed-valence state in the chain via a Peierls distortion. However, it is affected by the xy component in the dz^2 ($2z^2$-x^2-y^2) orbital. In other words, the changing approach from the lone pair

of NH_2 group to the Pd center gives perturbation to the on-site Coulomb repulsion (U in the dz^2 orbital). Significantly, cptn ligand, which has a weak ligand field because of distortion by cyclopentane moiety, decreases U on Pd ion and changes the relation of $S > U$ compared to Pd complex with ethylenediamine ligand. Actually, $[Pd(cptn)_2Br]Br_2$ at 260 K is in the CDW state; even though the Pd-Pd distance (or a) of $[Pd(cptn)_2Br]Br_2$ is 5.25 A, which is on the borderline of the Pd-Pd distance between CDW and MH states for the Pd complex with ethylenediamine ligand and alkyl chain. On the other hand, the d value is a relative value between a and Δ; therefore, it is comparable among compounds.

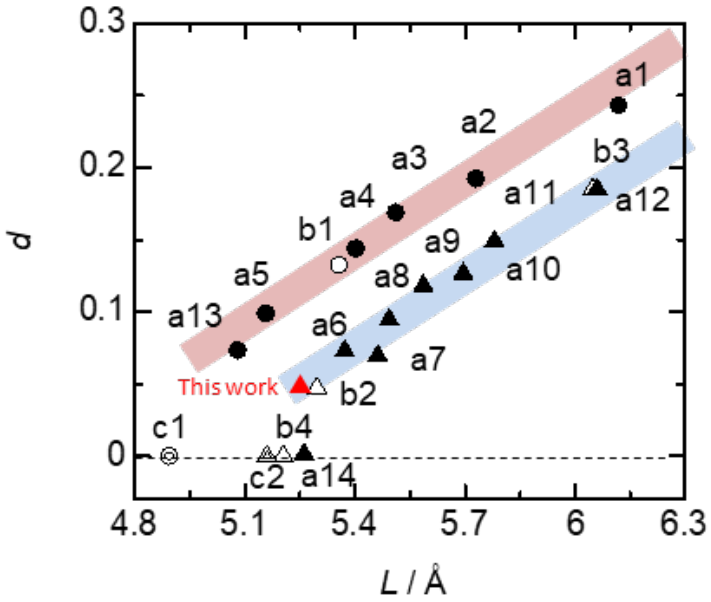

Figure S7. Correlation between d (= $(l_2 - l_1)$/L, where $l_2 = d(M^{II}\cdots X)$ and $l_1 = d(M^{IV}–X)$) and L (M–X–M distance). Circles and triangles represent Cl- and Br-bridged MX chains, respectively. Filled, hollow, and double markers show Pt-, Pd-, and Ni-based MX chains, respectively. Red color represents the this work. Data are shown for $[Pt(en)_2Cl](ReO_4)_2$ (a1),[S1] $[Pt(chxn)_2Cl](ClO_4)_2$ (a2),[S2] $[Pt\text{-}(pn)_2Cl](ClO_4)_2$ (a3),[S3] $[Pt(en)_2Cl](ClO_4)_2$ (a4),[S4] $[Pt\text{-}(chxn)_2Cl]Cl_2$ (a5),[S5] $[Pt(chxn)_2Br]Br_2$ (a6),[S6] $[Pt(tn)_2Br](BF_4)_2$ (a7),[S3] $[Pt(en)_2Br](ClO_4)_2$-1 (a8),[S2] $[Pt(etn)_4Br]Br_2$ (a9),[S3] $[Pt\text{-}(en)_2Br](ClO_4)_2$-2 (a10),[S7] $[Pt(chxn)_2Br](ClO_4)_2$ (a11),[S8] $[Pt\text{-}(en)_2Br](ReO_4)_2$ (a12),[S3] $[Pd(en)_2Cl](ClO_4)_2$ (b1),[S9] $[Pd\text{-}(chxn)_2Br]Br_2$ (b2),[S1] $[Pd(en)_2Br](ReO_4)_2$ (b3),[S2] $[Ni(chxn)_2Cl]\text{-}Cl_2$ (c1),[S2] $[Ni(chxn)_2Br]Br_2$ (c2),[S2] $[Pt(dabdOH)_2Cl]Cl_2$,[S10] $[Pt(dabdOH)_2Br]Br_2$,[S18] and $[Pd(dabdOH)_2Br]Br_2$.[S19] Pink and blue highlight lines are guides for the eyes for each X– ion. (chxn = cyclohexanediamine; en = ethylenediamine; etn = ethylamine; tn = 1,3-diaminopropane, pn = 1,2-diaminopropane).

Temperature dependence

Several measurements at different temperature were performed in order to establish a temperature dependence of the CDW correlation length in order to check if there was a phase transition from MH to CDW at low temperature. There were several hints of a transition at around 120K from raman, optical spectroscopy and susceptibility measurement.

As expected the intensity of the diffuse scatterings gradually weakened upon cooling and mostly disappeared at 100 K, indicating that the electronic state is changing from CDW to MH state gradually. (figure S8) But data reproducibility was very poor

For any temperature that we checked we observed in the first minutes, the diffuse scattering as diffuse rods and sharper peaks (but not bragg peaks). We observed that the sharp peaks in the diffuse scattering responsible for the plane to plane correlation rapidly disappear under Xray irradiation. After 15 minutes of data collection, we could only see the diffuse planes and no more the peaks. The reason might come from xray photon absorption on the palladium that could destabilized the coulomb coupling responsible for the antiphase ordering and therefore the 3D ordering. We guess that after longer exposure it could destabilize also the 2D-CDW and may be the reason for bad reproducibility in the temperature dependence measurement. We had to make a complete data collection at each temperature and the sample has to be exposed for at least 3 minutes

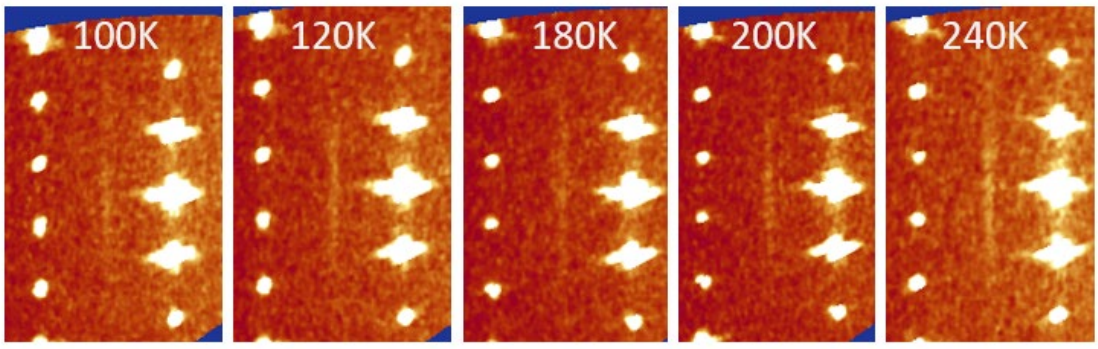

Figure S8 : Temperature dependence of the diffuse scattering.

[S1] S. Kumagai, S. Takaishi, M. Gao, H. Iguchi, B. K. Breedlove, M. Yamashita, *Inorg. Chem.* **2018**, *57*, 3775– 3781

[S2] H. Okamoto, M. Yamashita, *Bull. Chem. Soc. Jpn.* **1998**, *71*, 2023– 2039.

[S3] R. J. H. Clark, *Advances in Infrared and Raman Spectroscopy Volume 11*; R. J. H. Clark, R. E. Hester; Wiley: Hayden, **1984**; Chapter 3.

[S4] N. Matsumoto, M. Yamashita, I. Ueda, S. Kida, *Mem. Fac. Sci., Kyushu Univ., Ser. C* **1978**, *11*, 209– 216.

[S5] K. P. Larsen, H. Toftlund, E. Näsäkkälä, A. Kjekshus, T. Rakke, A. F. Andresen, *Acta Chem. Scand.* **1977**, *31a*, 182– 186.

[S6] H. Okamoto, K. Toriumi, T. Mitani, M. Yamashita, *Phys. Rev. B: Condens. Matter Mater. Phys.* **1990**, *42*, 10381– 10387.

[S7] K. Toriumi, M. Yamashita, S. Kurita, I. Murase, T. Ito, *Acta Crystallogr Sect B* **1993**, *49*, 497– 506.

[S8] B. Scott, S. P. Love, G. S. Kanner, S. R. Johnson, M. P. Wilkerson, M. Berkey, A. Swanson, B. I. Saxena, X. Z. Huang, A. R. Bishop, *J. Mol. Struct.* **1995**, *356*, 207– 229.

[S9] A. L. Beauchamp, D. Layek, T. Theophanides, *Acta Crystallogr., Sect. B: Struct. Crystallogr. Cryst. Chem.* **1982**, *38*, 1158– 1164.

[S10] M. Rasel. Mian, H. Iguchi, S. Takaishi, U. Afrin, T. Miyamoto, H. Okamoto, M. Yamashita, *Inorg. Chem.* **2019**, *58*, 114−120.

[S11] M. Rasel Mian, H. Iguchi, S. Takaishi, H. Murasugi, T. Miyamoto, H. Okamoto, H. Tanaka, S. Kuroda, B. K. Breedlove, M. Yamashita, *J. Am. Chem. Soc.* **2017**, *139*, 6562−6565.